# Effect of Temperature, Rate, and Molecular Weight on the Failure Behavior of Soft Block Copoly(ether-ester) Thermoplastic Elastomers

**Simone Sbrescia[1], Jianzhu Ju[2], Costantino Creton[2], Tom Engels[3], Michelle Seitz[3]**

[1] Bio and Soft Matter Division (BSMA), Institute of Condensed Matter and Nanosciences (IMCN), Université Catholique de Louvain, B-1348 Louvain-la-Neuve, Belgium;

[2] Laboratoire Sciences et Ingénierie de la Matière Molle, ESPCI Paris, PSL University, CNRS, Sorbonne Université, Paris, France;

[3] DSM Materials Science Center, Urmonderbaan, 6167 RD Geleen The Netherlands;

## Supplemental Information

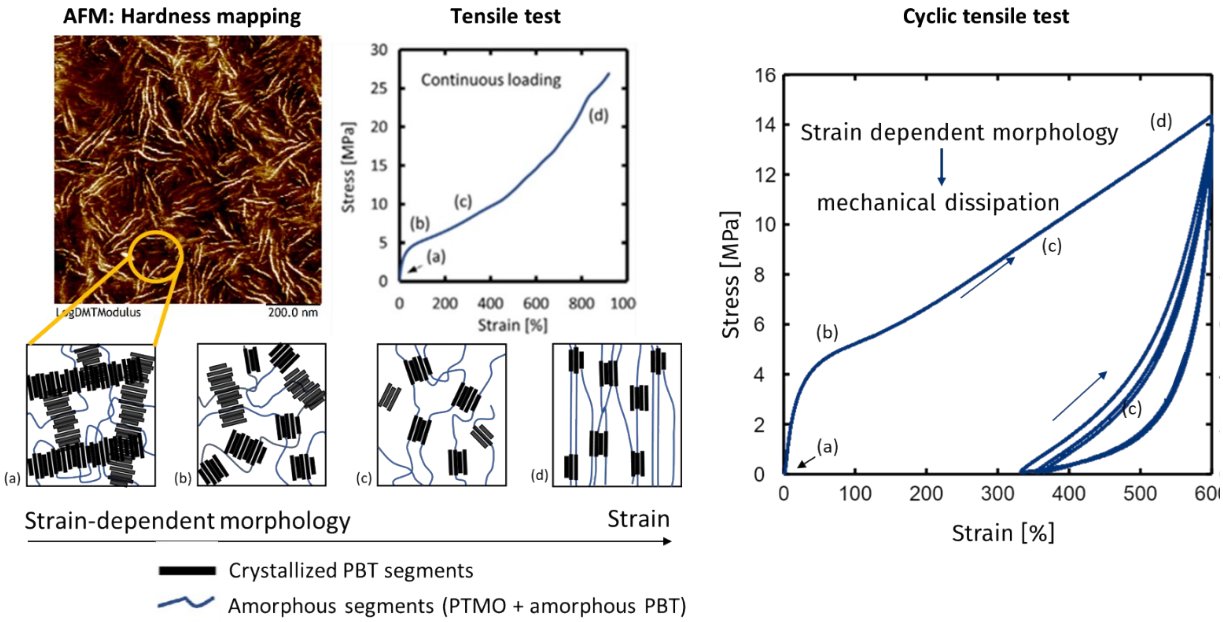


**Figure S1:** Description of the microstructure of the copoly(ether-ester) TPEs under study, including the changes it undergoes as the material is stretched. On the top-left, an AFM hardness mapping of the surface of one tested sample shows the high aspect ratio of the PBT crystals forming an interlocked hard phase. Details on the method for the AFM can be found in our previous study [20]. On the top-center, a stress-strain plot performed at RT on the low-Mw sample. Here, the different stages in strain where the microstructure is expected to change are highlighted. The corresponding changes are depicted on the bottom-left of the figure. On the right, a cyclic tensile test where the multiple cycles following the first one is done at the same level of strain. This last part substantiates the irreversible changes occurring to the microstructure, where the first cycle shows large hysteresis and plasticity, while the subsequent cycles exhibit considerably more elastic behavior, which remains relatively constant as the number of stretching cycles increases. Figure is rearranged from figures in our previous study [20].

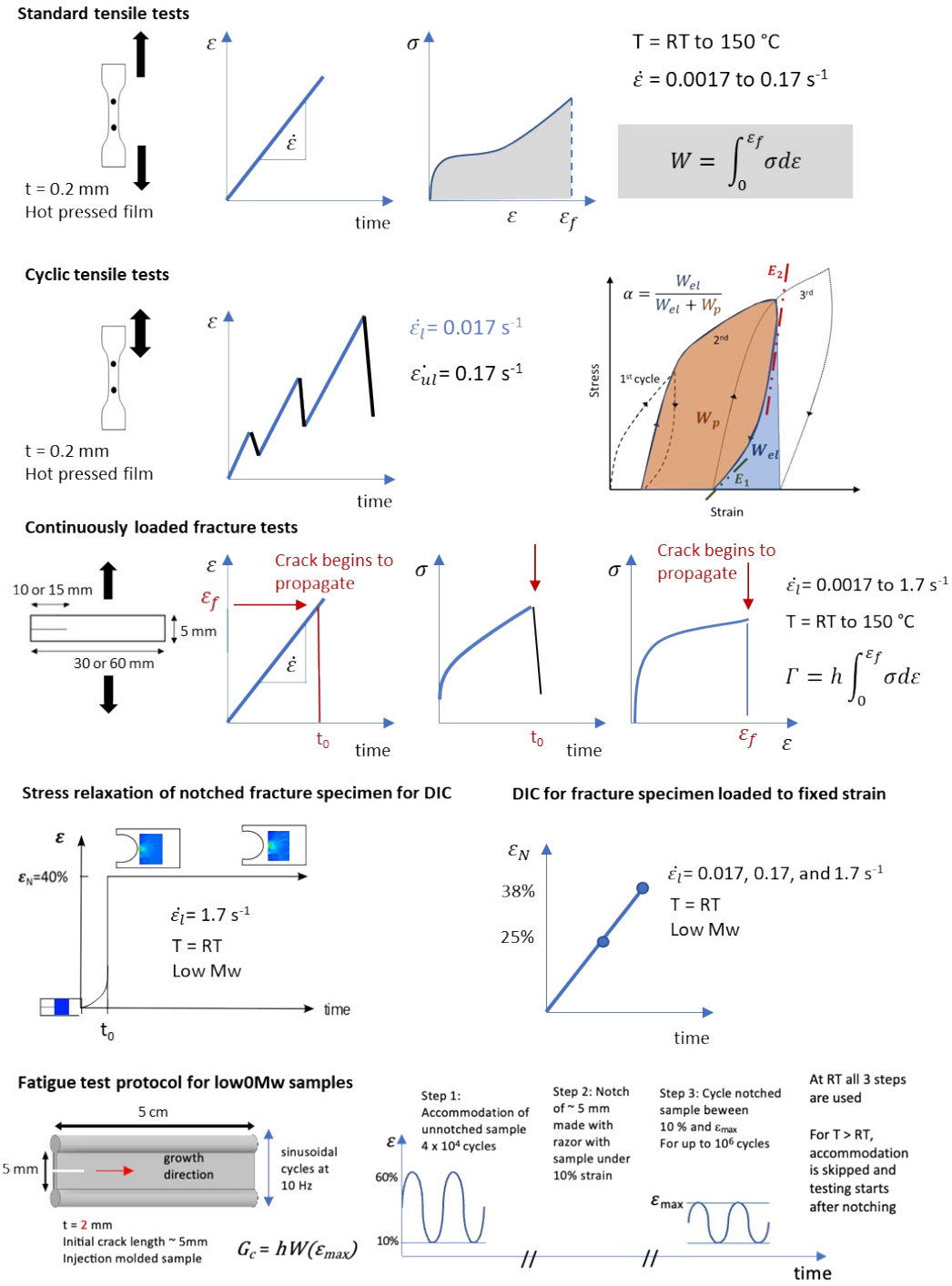


**Figure S2:** General overview of the testing methods, samples geometries and definitions of the variables.

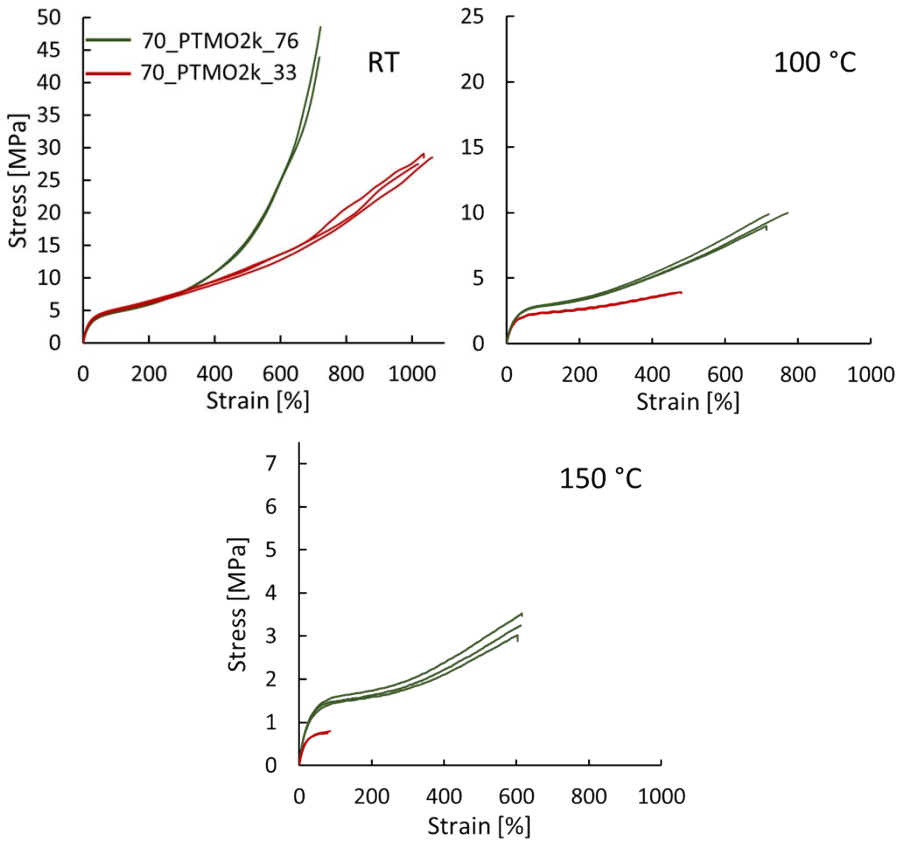


**Figure S3:** Engineering stress-strain curve performed, from left to right, at RT, 100 °C, and 150 °C, at $\dot{\varepsilon} = 0.17\ s^{-1}$.

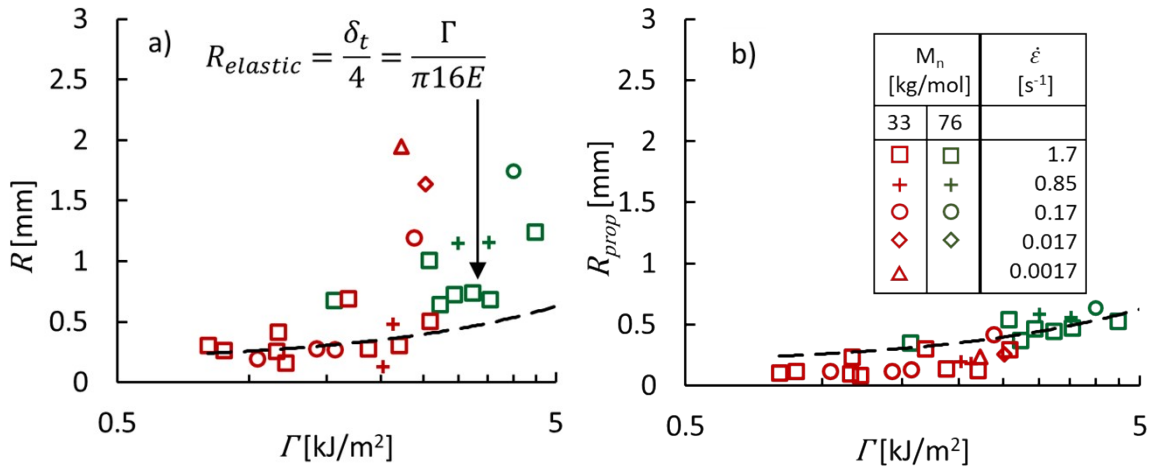


**Figure S4:** Radius of the crack tip right before crack propagation, $R$, (a) and during propagation, $R_{prop}$ (b) calculated via parabolic fit of the crack tip.

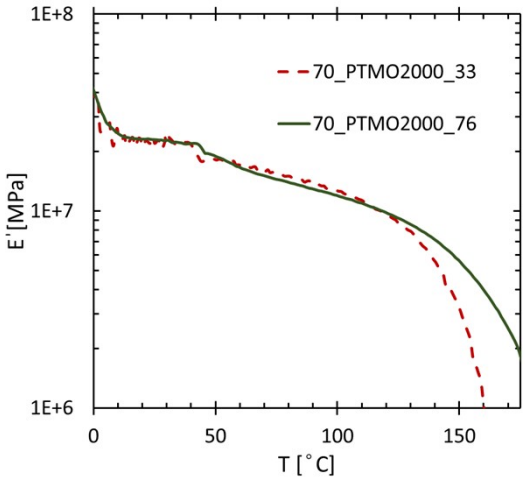


**Figure S5:** Storage modulus of the samples 70_PTMO2k_33 and 70_PTMO2k_76. Rectangular shaped samples (40 mm long, 2 mm wide) punched out from the 200 µm hot-pressed films are tested in tension at heating rates of 5 °C/min and at a constant frequency of 1 Hz. The elastic modulus is measured from DMTA rather than being calculated from tensile tests for convenience and increased accuracy.

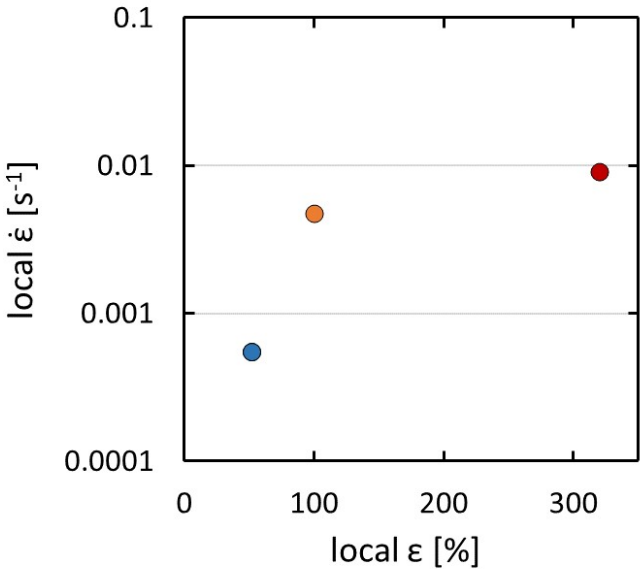


**Figure S6:** Local strain-rate calculated from the changes in the local strain Vs time during the stress relaxation test (Figure 10).

**Derivation of the relationship between $R_{LEFM}$ and $\delta_t$**

The equation $R_{LEFM} = \delta_t /4$ used in Figure 7 derives from the work of Mac Donald *et al* [54]. $\delta_t$ is determined by the intersection of lines at 45° from the origin of the parabola. The distance between the intersecting line of length $\delta_t$ and the origin of the parabola is shown to be $\delta_t/2$.

The curvature of the parabola $y = ax^2$ with origin placed at the crack tip center can be determined by substituting $y = \delta_t/2$, $x = \delta_t/2$, and $R_{LEFM} = 1/|2a|$.

Substituting and solving for $R_{LEFM}$ leads to $R_{LEFM} = \delta_t/4$.

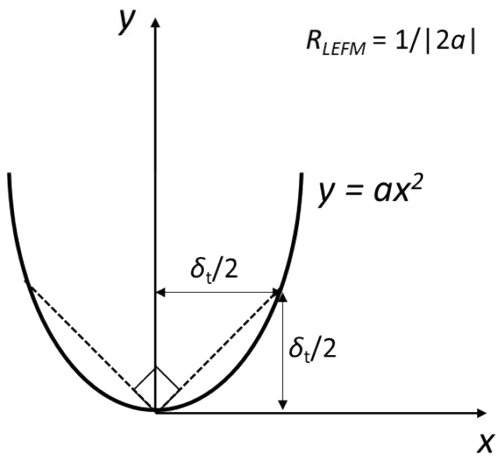

**Table S1-a – Acquired data on PS geometry**

Averages of the failure strain ($\varepsilon_f$), failure stress ($\sigma_f$), $\Gamma$, and crack-propagation speed ($v$) collected from the tests with notched samples in PS geometry at different T's and $\dot{\varepsilon}$'s.

| Sample | T | ε | $\varepsilon_f$ | $\sigma_f$ | $\Gamma$ | $\Gamma/E$ | $\Gamma_{local}$ | $v$ |
|---|---|---|---|---|---|---|---|---|
| | °C | $s^{-1}$ | % | MPa | $kJ/m^2$ | mm | $kJ/m^2$ | mm/s |
| **70_PTMO2k_33** | RT | 1.7 | 73.7 | 4.2 | 11.9 | 0.51 | 6.3 | 519 |
| | 75 | 1.7 | 314.8 | 1.7 | 2.2 | 0.15 | 1.2 | 314 |
| | | 0.17 | 206.8 | 2.7 | 24.7 | 1.65 | 11.3 | |
| | 100 | 1.7 | 29.7 | 1.2 | 1.2 | 0.09 | 0.6 | 243 |
| | | 0.85 | 48.7 | 1.3 | 2.1 | 0.16 | 1.1 | 267 |
| | | 0.17 | 39.1 | 1.1 | 1.5 | 0.11 | 0.8 | 196 |
| | | 0.017 | 136.1 | 1.8 | 12.2 | 0.94 | 6.4 | |
| | 125 | 1.7 | 39.2 | 1.2 | 1.1 | 0.12 | 0.6 | 219 |
| | | 0.17 | 54.0 | 0.8 | 1.7 | 0.19 | 0.9 | 183 |
| | | 0.017 | 92.1 | 1.0 | 3.1 | 0.34 | 1.6 | 295 |
| | | 0.0017 | 65.8 | 0.8 | 2.4 | 0.27 | 1.3 | 229 |
| **70_PTMO2k_76** | RT | 1.7 | 81.0 | 4.3 | 13.6 | 0.59 | 8.5 | 488 |
| | | 0.17 | 231.1 | 5.2 | 51.8 | 2.25 | 32.4 | 485 |
| | 75 | 1.7 | 85.0 | 3.3 | 11.5 | 0.79 | 7.2 | 327 |
| | | 0.17 | 337.9 | 4.9 | 66.7 | 4.60 | 41.7 | |
| | 100 | 1.7 | 72.7 | 2.9 | 8.2 | 0.68 | 4.2 | 235 |
| | | 0.85 | 89.6 | 2.5 | 8.0 | 0.67 | 2.2 | 246. |
| | | | 330.3 | 3.9 | 52.6 | 4.34 | 32.9 | |
| | | 0.17 | 322.3 | 3.2 | 47.6 | 3.93 | 29.7 | |
| | 125 | 1.7 | 58.4 | 2.2 | 3.7 | 0.41 | 2.1 | 167 |
| | | 0.85 | 57.1 | 1.7 | 3.3 | 0.37 | 2.0 | 165 |
| | | 0.17 | 427.0 | 2.9 | 48.7 | 5.4 | 30.5 | |
| | 150 | 1.7 | 47.8 | 1.2 | 2.1 | 0.39 | 1.4 | 121 |
| | | 0.17 | 92.1 | 1.2 | 5.0 | 0.92 | 3.1 | 124 |
| | | 0.017 | 148.3 | 1.0 | 6.9 | 1.28 | 4.9 | 151 |
| | | 0.0017 | 266.7 | 1.2 | 13.0 | 2.40 | 9.2 | |

The cells where the crack-propagation value is missing correspond to the experimental conditions at which the crack propagated in the direction perpendicular to the stretching direction, for which the crack-propagation speed was not calculated. The investigated $\dot{\varepsilon}$'s range from $0.0017s^{-1}$ to $1.7s^{-1}$, however, if at a given ε the crack blunted too much and the crack propagated perpendicularly to the stretching direction, the lower $\dot{\varepsilon}$'s were not investigated. The uncertainty on the directly measured values are shown in Table S1-b.

**Table S1-b – Uncertainty on the acquired data on PS geometry**

Standard deviation relative to the values shown in Table S1-a.

| Sample | T | ε | $\varepsilon_f$ | $\sigma_f$ | $\Gamma$ | $v$ |
|---|---|---|---|---|---|---|
| | °C | $s^{-1}$ | % | MPa | $kJ/m^2$ | mm/s |
| **70_PTMO2k_33** | RT | 1.7 | 1.0 | 0.4 | 1.1 | 9.6 |
| | 75 | 1.7 | 1.9 | 0.1 | 0.4 | 26.8 |
| | | 0.17 | 76.7 | 0.7 | 10.7 | |
| | 100 | 1.7 | 2.9 | 0.1 | 0.0 | 4.1 |
| | | 0.85 | 3.2 | 0.1 | 0.1 | 3.9 |
| | | 0.17 | 2.3 | 0.0 | 0.1 | 11.9 |
| | | 0.017 | 35.5 | 0.0 | 3.7 | |
| | 125 | 1.7 | 8.0 | 0.4 | 0.4 | 19.5 |
| | | 0.17 | 23.1 | 0.0 | 0.9 | 46.6 |
| | | 0.017 | 29.1 | 0.2 | 1.2 | 11.0 |
| | | 0.0017 | 4.2 | 0.0 | 0.3 | |
| **70_PTMO2k_76** | RT | 1.7 | 14.7 | 0.4 | 4.2 | 20.1 |
| | | 0.17 | 16.4 | 0.4 | 0.3 | 6.1 |
| | 75 | 1.7 | 3.6 | 0.0 | 0.9 | 1.2 |
| | | 0.17 | 90.2 | 0.9 | 26.8 | |
| | 100 | 1.7 | 13.3 | 0.3 | 3.1 | 7.0 |
| | | 0.85 | 170.2 | 1 | 31.5 | |
| | | 0.17 | 146.3 | 0.0 | 25.9 | |
| | 125 | 1.7 | 7.9 | 0.4 | 0.8 | 1.2 |
| | | 0.85 | 10.4 | 0.1 | 0.4 | 4.6 |
| | | 0.17 | 14.5 | 0.1 | 1.9 | |
| | 150 | 1.7 | 7.1 | 0.2 | 0.7 | 17.0 |
| | | 0.17 | 8.9 | 0.2 | 0.8 | 1.5 |
| | | 0.017 | 4.3 | 0.0 | 1.4 | 3.9 |
| | | 0.0017 | 45.8 | 0.1 | 1.7 | |

**Table S2 – Acquired additional data from standard tensile test**

Averages of the failure strain ($\varepsilon_f$), failure stress ($\sigma_f$), yield stress ($\sigma_y$), $W$, calculated from the standard tensile tests at different T's and $\dot{\varepsilon}$'s.

| Sample | T | ε | $\varepsilon_f$ | $\sigma_f$ | $\sigma_y$ | $W$ |
|---|---|---|---|---|---|---|
| | °C | $s^{-1}$ | % | MPa | MPa | $MJ/m^3$ |
| **70_PTMO2k_33** | RT | 0.17 | 1037.7 ± 20.1 | 28.3 ± 0.8 | 4.4 | 136.5 ± 4.7 |
| | 75 | 0.17 | 655.5 ± 43.1 | 6.4 ± 0.1 | 2.7 | 28.9 ± 2.3 |
| | 100 | 0.17 | 470.5 ± 12.0 | 3.9 ± 0.1 | 2.1 | 13.0 ± 0.9 |
| | | 0.017 | 395.6 ± 46.9 | 3.3 ± 0.2 | 1.9 | 9.6 ± 1.3 |
| | | 0.0017 | 338.7 ± 5.9 | 2.7 ± 0.1 | 1.7 | 7.0 ± 0.4 |
| | 125 | 0.17 | 449.0 ± 36.8 | 2.2 ± 0.1 | 1.5 | 7.8 ± 0.4 |
| **70_PTMO2k_76** | RT | 0.17 | 713.5 ± 12.0 | 45.6 ± 3.8 | 4.0 | 86.5 ± 4.2 |
| | 75 | 0.17 | 818.0 ± 103.2 | 13.7 ± 2.8 | 2.8 | 58.3 ± 16.9 |
| | 100 | 0.17 | 732.7 ± 33.7 | 9.6 ± 0.6 | 2.5 | 38.2 ± 3.0 |
| | 125 | 0.17 | 618.7 ± 50.8 | 5.4 ± 0.6 | 1.9 | 20.2 ± 3.2 |
| | 150 | 0.17 | 607.7 ± 6.7 | 3.2 ± 0.3 | 1.3 | 12.3 ± 1.2 |

As there is no local maximum in the stress-strain curves to represent $\sigma_y$, the latter is taken as the stress at ε = 50%. $E_1$ and $E_2$ are calculated from the cyclic tensile tests as shown in Figure 1. The former corresponds to the unloading modulus calculated from the cycle corresponding to an applied strain of 150%, the latter to the highest applied strain measured.

**Table S3-a – Acquired additional data from cyclic tensile tests**

Averages of $E_1$ and $E_2$ calculated from the cyclic tensile tests as shown in Figure 1. The former corresponds to the unloading modulus calculated from the cycle corresponding to an applied strain of 150%, the latter to the highest applied strain measured ($\varepsilon_{max}$). The calculation of the moduli takes into account the changes in thickness of the samples with increasing deformation assuming volume conservation.

| Sample | T | $E_1$ | $E_2(\varepsilon_{max})$ | $\varepsilon_{max}$ |
|---|---|---|---|---|
| | °C | MPa | MPa | % |
| **70_PTMO2k_33** | RT | 5.8 | 330.3 | 550 |
| | 75 | 4.3 | 65.9 | 550 |
| | 100 | 2.3 | 25.1 | 350 |
| | 125 | 1.0 | 13.0 | 350 |
| **70_PTMO2k_76** | RT | 5.5 | 452.2 | 550 |
| | 75 | 4.0 | 211.0 | 750 |
| | 100 | 3.7 | 91.0 | 750 |
| | 125 | 1.2 | 31.2 | 450 |
| | 150 | 1.2 | 16.0 | 550 |